Nuclei of the Pt(111) Network Reconstruction Created by Single Ion Impacts

Christian Teichert,* Michael Hohage, Thomas Michely, and George Comsa
Institut für Grenzflächenforschung und Vakuumphysik, KFA-Forschungszentrum Jülich, D-52425 Jülich, Germany
(Received 7 September 1993)

The surface damage induced on Pt(111) by single rare gas ion impacts with energies down to a few hundred eV has been investigated by scanning tunneling microscopy. In addition to craters and adatom islands there are also characteristic reconstruction patterns in the vicinity of the ion impacts. It is demonstrated that these reconstructed areas are nuclei of the reconstruction network which has been discovered recently to be induced by Pt vapor phase deposition. The formation of these nuclei by ion bombardment is discussed in terms of currently used damage generation models.

PACS numbers: 61.80.Jh, 61.16.Ch, 68.35.Bs, 68.35.Fx

The imaging of surface damage by single ion impacts on layered materials [1] and on silicon [2], i.e., on materials which exhibit only little damage annealing, has become possible in the last few years by scanning tunneling microscopy (STM). However, information on defect patterns generated by single ion impacts on metals, which exhibit strong damage annealing even at ambient temperature, has so far not been obtained by STM but mainly by field ion microscopy (FIM) and transmission electron microscopy (TEM) [3,4]. The applicability of these methods is restricted either by sample geometry and material strength requirements (FIM) or by limited resolution (TEM). Since the simulation of impact events and their morphological effects on surfaces is most advanced for metals [5–7], additional experimental tools for the investigation of single ion impacts on metals are highly desirable.

We show here that by STM it is possible to record the fingerprints of single ion impacts on Pt(111) down to primary ion energies of a few hundred eV. In addition to surface craters and adatom islands surrounding the craters, most surprisingly characteristic reconstruction patterns are also observed. According to first principles calculations Pt(111) exhibits tensile surface excess stress —a positive strain derivative—and thus is close to an instability towards reconstruction by insertion of extra atoms into the surface layer [8]. In fact Pt(111) forms a reconstructed equilibrium phase above 1330 K with an increased atomic density in the surface layer [9]. Down to 400 K a metastable phase with a characteristic reconstruction network can be induced in a supersaturated Pt vapor environment, which supplies the extra atoms inserted [10]. The observed reconstruction patterns originating from single ion impacts are demonstrated here to be again a consequence of the instability of the Pt(111) surface layer towards an increase in atomic density and to be nuclei of the network reconstruction. These results together with conclusions from effective medium theory [11] allow one to derive a model for the nucleation of the reconstruction by the supersaturated Pt vapor. This model is then used to assess the possible role of interstitials and of collective mechanisms in the creation of the reconstruction nuclei by ion bombardment.

The experiments were performed in a UHV chamber equipped with a differentially pumped ion gun, a Pt sublimator, an STM, and standard surface analysis facilities [12]. The ion bombardment was performed under normal incidence at various substrate temperatures between 150 and 450 K. The specified ion doses were determined by a Faraday cup and cross checked with the number of impacts visible in STM per unit area. The temperature of STM investigation was typically room temperature (RT). Only for bombardment below RT was the temperature kept low to prevent diffusional changes of the morphology.

Figure 1(a) represents the surface morphology after a dose of 4.1×10^{15} ions/m^2 of 5 keV Xe^+ ions at 300 K, corresponding to an average of 17 impacts on a surface area as on the topograph. Three distinct types of defects are clearly visible: (i) vacancy islands (craters), (ii) adatom islands of monatomic height, and (iii) ringlike to triangular corrugation line features with a height of 0.2 Å (for convenience called "loops" in the following). Within the statistical fluctuations the number of craters corresponds to the number of impacts expected from the Faraday cup ion current measurement. *Thus every visible crater is attributed to a single ion impact.* The number of vacancies within each crater has been estimated to be between 10 and 20 [13]. This corresponds roughly to the sputtering yield of 14.5 for 5 keV Xe^+ determined by the method described in Ref. [14]. Although the impacts scatter considerably in their appearance, they can be classified in one of the following groups [see Fig. 1(a)]: crater associated with 1 adatom island(s) (~70%), 2 adatom island(s) and loop (~20%), and 3 with loop only (~10%). The average number of adatoms created per impact is 65 [15]. The average center-to-center separation between an adatom island and a crater is 22 Å. The average center-to-center distance between a loop that can be attributed unambiguously to a single impact and a crater is 25 Å. Those loops contain 18 ± 5 extra atoms in the surface layer [16]. Sometimes we observed larger and more structured loops of the same 0.2 Å height situated between several impacts [see 4 in Fig. 1(a)], or loops

0031-9007/94/72(11)/1682(4)$06.00

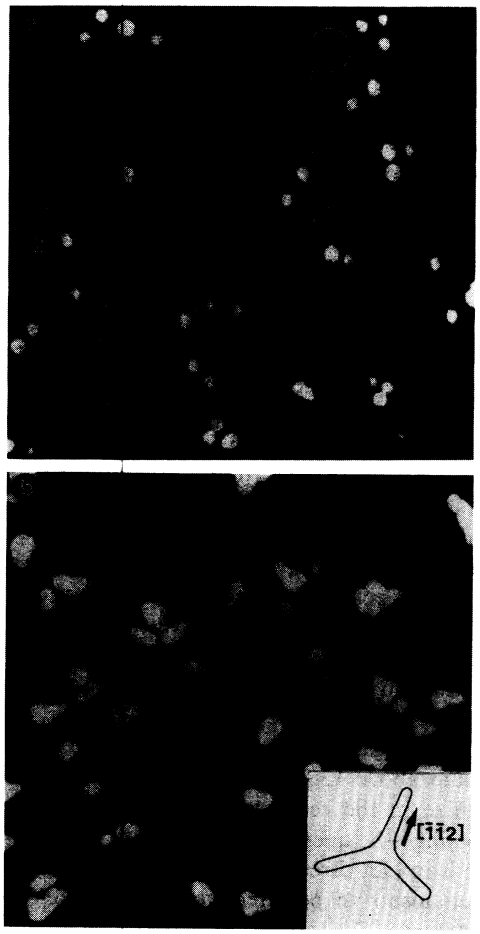

FIG. 1. (a) STM topograph (650 Å×650 Å, illumination from the left) obtained after a dose of 4.1×10^{15} 5 keV Xe^+ ions/m^2 at 300 K. The defect patterns 1 to 5 are discussed in the text. (b) Topograph (1100 Å×1100 Å, grey scale) taken after a dose of 1.9×10^{15} 5 keV Xe^+ ions/m^2 at 300 K and subsequent Pt vapor phase deposition of 0.08 ML at 300 K with a deposition rate of 2.6×10^{-4} ML/s. Inset: scheme of a single dark star.

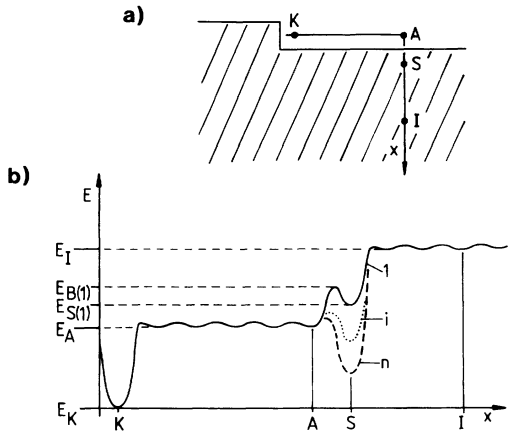

FIG. 2. (a) Coordinate x for a path from kink site K over terrace site A, surface interstitial site S to bulk interstitial site I. (b) Potential energy of an atom on a path along x. The well-depth energy E_S and the barrier height E_B decrease with increasing number of extra atoms in the surface layer (first atom: solid curve; ith atom: dotted curve; nth atom: dashed curve).

situated further away from craters with often somewhat smaller sizes [see 5 in Fig. 1(a)].

In order to determine the nature of the loops we performed the following experiment: After a prebombardment with about half the ion dose as in Fig. 1(a) at 300 K, we deposited 0.08 ML of Pt from the vapor phase at a rate of 2.6×10^{-4} ML/s (ML denotes monolayer) at 300 K [see Fig. 1(b)]. The resulting morphology exhibits a clear reconstruction network (compare with Fig. 2 in Ref. [10]). All over the surface there are well developed dark stars [see inset, Fig. 1(b)] which are already partially connected forming bright spots. Proceeding like this, the reconstruction network could be generated down to temperatures of 150 K. In contrast, it was *never* possible to generate a reconstruction network solely by vapor phase deposition at temperatures *below 400 K*. We may thus conclude that (1) the bombardment-induced loops are nuclei of the network reconstruction and (2) the further growth of reconstruction nuclei to a reconstruction network by inserting atoms supplied from the vapor phase is possible at much lower temperatures (≤ 150 K) than the nucleation from the vapor phase (>400 K); i.e., the vapor-deposited Pt adatoms have to overcome a much higher activation barrier for creating a reconstruction nucleus than for further growth of a nucleus.

It has been demonstrated that once formed in the presence of Pt vapor the reconstruction network remains in a metastable state up to 700 K even in the absence of Pt vapor [10]. At 700 K the network decays and after a couple of minutes only reconstruction loops—similar to those in Fig. 1(a)—are left behind. With continued annealing they eventually also disappear.

These observations together with results from effective medium theory [11] lead to a simple model for the nucleation of the reconstruction on an atomistic scale. A Pt atom deposited as adatom (A in Fig. 2) on the Pt(111) surface migrates on the terrace until it is incorporated into a kink site K of a step (for simplicity the nucleation of adatom islands is neglected). However, an adatom can also attempt to enter the first surface layer and become incorporated in the position S by overcoming a barrier of height $E_{B(1)}-E_A$. Once, the adatom has overcome the barrier, it is trapped as a *surface* interstitial in a potential well of depth $E_{B(1)}-E_{S(1)}$. Since for the first extra atom $E_{S(1)}>E_A$ [11], the atom will return to the adatom position A after a certain residence time and finally become incorporated in a kink site K. However, due to the high supersaturation of the surrounding Pt vapor a second adatom may join the surface interstitial before it has left S. This process is eased due to the strain field of the sur-

face interstitial reducing $E_{B(2)}-E_A$ compared to $E_{B(1)}-E_A$. Moreover the drop of the energy E_S for the second atom [11] (probably already below the adatom level E_A) gives rise to an enhanced lifetime of the surface interstitial dimer. In the presence of the supersaturated vapor the further increase of the number i of extra atoms becomes more and more probable because $E_{S(i)}$ drops with i [11] and also because $E_{B(i)}-E_A$ will reduce further with increasing i. The process repeats itself until the reconstruction loop is fully developed at about 15 incorporated extra atoms. At this point the energy per incorporated extra atom attains practically its lowest saturation value $E_{S(n)}$. During further growth the additionally incorporated atoms lead to the formation of the three rays of the dark star [see, e.g., Fig. 1(b) and inset]. This simple model of the nucleation of the reconstruction is in accord with all experimental observations so far: (i) The reconstruction cannot be nucleated below 400 K from the vapor phase since the probability to overcome $E_{B(1)}-E_A$ is negligible below that temperature; (ii) the surface is not reconstructed spontaneously since $E_K < E_{S(n)}$; (iii) the reconstruction decays above 700 K in the absence of the supersaturated Pt gas phase since the probability to overcome $E_{B(n)}-E_{S(n)}$ becomes significant and $E_K < E_{S(n)}$; (iv) the proximity of kink sites hinders the growth of the reconstruction; (v) no atoms are incorporated into deeper layers since $E_I > E_S$; (vi) once reconstruction nuclei are present, the further growth from vapor continues down to at least 150 K since $E_{B(n)}-E_A \ll E_{B(1)}-E_A$.

Let us now try to analyze the creation of reconstruction nuclei by ion impact, taking advantage of the model deduced above for the nucleation from gas phase (Fig. 2).

When an ion hits the solid a collision cascade is initiated, giving rise to a considerable number of energetic atoms. Atoms which receive a normal component of kinetic energy directed outward larger than a given threshold leave the crystal; they become sputtered. Surface vacancies remain behind. Atoms with less normal kinetic energy do not become sputtered, but may be pushed *onto* the surface layer and become adatoms [17]. Moreover, replacement collision sequences directed away from the cascade core create stable bulk interstitials in the surrounding, leaving bulk vacancies in the cascade core behind (Frenkel pairs). At $T > 30$ K the interstitials migrate thermally even after the impact energy has dissipated [18]. They either recombine with bulk vacancies —which are immobile up to 450 K in Pt [19]—or eventually approach the surface. During the collisional part of the damage production the Pt atoms approach the surface layer with energies well above thermal energies, whereas the migrating interstitials have only thermal energies. Thus they are trapped with high efficiency in the potential well of the surface layer position S. In contrast to adatoms, these bulk interstitials do *not* have to overcome a barrier to reach this position, i.e., to become surface interstitials. Since by one single ion impact a large number of interstitials is created at one time in a small volume [20]—building up locally an extreme supersaturation of interstitials—the probability of interstitials to nucleate in the surface layer and to create a loop is large. Most interstitials are created only a few 10 Å away from the vacancy-rich core [20] so that most loops nucleate close to the impact craters as observed experimentally. However, interstitials are also detected in distances of 100 Å or more [20] which explains why some loops are observed further away from impact craters. The particularly large loops situated between several impact sites [see 4 in Fig. 1(a)] result from the successive addition of interstitials that originated from nearby impacts to the loop created by the first impact.

This damage model, which involves the existence of a highly supersaturated gas of bulk interstitials that can easily reach the surface layer, offers a straightforward explanation of the phenomena described so far.

In view of the kinetic energies of the primary ions in the keV range, possible consequences of the thermal-spike phase in the damage evolution have to be considered [6]. Molecular dynamics simulations indicate that a thermal spike leading to the melt of a small volume during a few picoseconds following the impact [5] can be created at these ion energies. Since Pt(111) is reconstructed in equilibrium above 1330 K [9], the molten surface might recrystallize in the reconstructed state and—due to the rapid cooling—be quenched in this state.

There is in fact direct experimental evidence for collective mechanisms to be effective during 5 keV Xe^+ ion bombardment. The appearance of the damage around ion impact events at a fixed ion energy scatters considerably. We observe "large" impact events with up to 500 adatoms pushed onto the surface layer (three of these are presented in Fig. 3) [21]. This large amount of adatoms can hardly be explained in a purely collisional model but is in agreement with molecular dynamics simulations, which indicate that such amounts of molten material may be pushed onto the surface in a thermal spike [7]. Note, however, that no loops are found in the vicinity of these large events, in contrast to our "quenched reconstruction" speculation.

Nevertheless, collective effects like propagation of a shock wave from the spike [5] or local heating without

FIG. 3. 5 keV xenon impacts, each causing 400 to 600 atoms to become adatoms (260 Å×220 Å, right topograph: illumination from the left; others: grey scale). Note also a second layer adatom island in left topograph.

melting might be relevant for loop creation. One indication for the action of such a collective mechanism in loop creation is the observation of a threshold ion energy for the creation of reconstruction loops which appears to depend on the ion mass: The energies are 0.4, 0.6, and 0.8 keV for Xe^+, Ar^+, and Ne^+, respectively. These three threshold ion energies correspond to a threshold value of about 0.3 keV of the primary knock-on Pt atom, necessary for reconstruction loop creation. This rationalization indicates that a certain minimum energy density is necessary for the loop formation.

In summary, nuclei of the network reconstruction are created by single ion impacts on Pt(111). From the analysis of the growth behavior and from the results of effective medium theory [11] a nucleation model for the reconstruction consistent with the experimental results is proposed. The experimental results on the ion impact creation of reconstruction loops indicate that one of the mechanisms involved is the supply of interstitials from the supersaturated interstitial gas to the surface layer. Effects attributed to thermal spikes are also found to influence the surface morphology. However, the role played by collective mechanisms in the loop creation could not be established on the basis of these experiments alone but requires molecular dynamics simulations.

Quantitative comparisons of the damage patterns of keV ion impacts predicted by molecular dynamics simulations with those obtained by STM will possibly open new ways for the understanding of the ion-surface interaction. Moreover, keV ion impact analysis by STM might also be a tool for other surfaces with tensile excess stress to uncover whether an instability towards reconstruction is present [8].

The authors gratefully acknowledge clarifying discussions with Uffe Littmark, Robert Averback, P. Ehrhardt, and W. Schilling as well as the critical reading of the manuscript by Stefanie Esch. One of us (C.T.) acknowledges a fellowship of the Alfried Krupp von Bohlen und Halbach Foundation and support from the Alexander von Humboldt Foundation.

---

*Present address: University of Wisconsin-Madison, Department of Materials Science and Engineering, 1509 University Avenue, Madison, WI 53706.

[1] I. H. Wilson, N. J. Zheng, U. Knipping, and I. S. T. Tsong, Appl. Phys. Lett. **53**, 2039 (1988); L. Porte, M. Phaner, C.H. de Villeneuve, N. Moncoffre, and J. Tousset, Nucl. Instrum. Methods Phys. Res., Sect. B **44**, 116 (1989); R. Coratger, A. Claverie, A. Chahboun, V. Landry, F. Ajustron, and J. Beauvillain, Surf. Sci. **262**, 208 (1992); G. M. Shed and P. E. Russell, J. Vac. Sci. Technol. A **9**, 1261 (1991).

[2] I. H. Wilson, N. J. Zheng, U. Knipping, and I. S. T. Tsong, Phys. Rev. B **38**, 8444 (1988); H. J. W. Zandvliet, H. B. Elswijk, E. J. van Loenen, and I. S. T. Tsong, Phys. Rev. B **46**, 7581 (1992).

[3] D. Pramanik and D. N. Seidmann, J. Appl. Phys. **54**, 6352 (1986).

[4] K. L. Merkle and W. Jäger, Philos. Mag. A **44**, 741 (1981).

[5] T. Diaz de la Rubia, R. S. Averback, and Horngming Hseih, J. Mater. Res. **4**, 579 (1989).

[6] W. Schilling and H. Ullmaier, in *Physics of Radiation Damage in Metals*, Materials Science and Technology Vol. 10, edited by R. W. Cahn, P. Haasen, and K. Kramer (Verlag Chemie, New York, 1993).

[7] R. Averback and M. Ghaly, Nucl. Instrum. Methods Phys. Res., Sect. B (to be published).

[8] R. J. Needs, M. J. Godfrey, and M. Mansfield, Surf. Sci. **242**, 215 (1991).

[9] A. R. Sandy, S. G. J. Mochrie, D. M. Zehner, G. Grübel, K. G. Huang, and D. Gibbs, Phys. Rev. Lett. **68**, 2192 (1992).

[10] M. Bott, M. Hohage, Th. Michely, and G. Comsa, Phys. Rev. Lett. **70**, 1489 (1993).

[11] J. Jacobsen, Eksamensprojekt, Lyngby, 1993 (unpublished); J. Jacobsen, K. W. Jacobsen, and P. Stotlze (to be published).

[12] Th. Michely, Report No. Jül-Bericht 2569, Forschungszentrum Jülich, 1991 (unpublished).

[13] The number of vacancies in a crater is estimated by assuming the steepest possible walls compatible with the solid-on-solid condition, i.e., by assuming that the crater walls are bounded by {111} facets.

[14] Th. Michely and G. Comsa, Nucl. Instrum. Methods Phys. Res., Sect. B **82**, 207 (1993).

[15] In order to preserve the mass balance and in agreement with annealing experiments, the material of the adatom islands is counterbalanced by a corresponding number of subsurface vacancies.

[16] The number of extra atoms in the surface layer within a loop is determined by the measurement of the length of the corrugation line. A dense-packed atomic row along a corrugation line contains 0.5 extra atoms (see also Ref. [10]).

[17] R. P. Webb and D. E. Harrison, Jr., Phys. Rev. Lett. **50**, 1478 (1983); Th. Michely and G. Comsa, Phys. Rev. B **44**, 862 (1991).

[18] H. J. Dibbert, K. Sonnenberg, W. Schilling, and U. Dedek, Rad. Eff. **15**, 115 (1972).

[19] K. Sonnenberg, W. Schilling, K. Mika, and K. Dettmann, Rad. Eff. **16**, 65 (1972).

[20] D. N. Seidmann, R. S. Averback, and R. Benedek, Phys. Status Solidi (b) **144**, 85 (1987).

[21] It does not change the following arguments if these events are due to Xe^{++} ions.

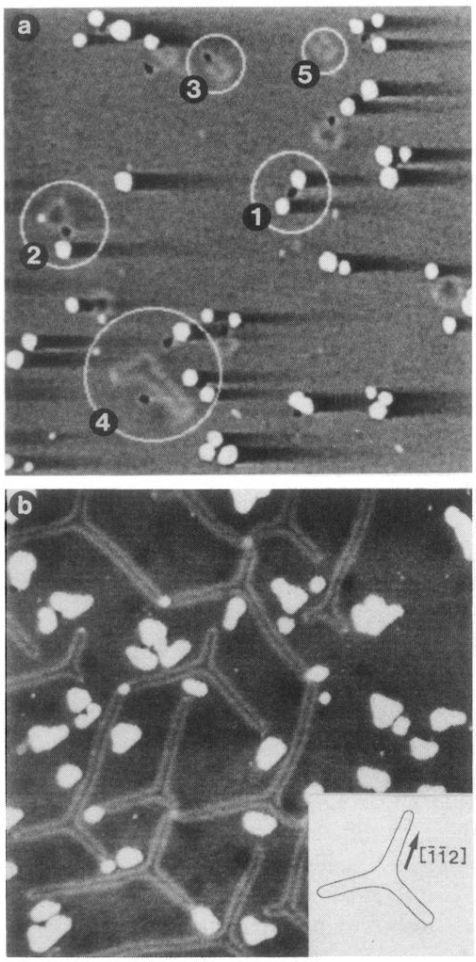

FIG. 1. (a) STM topograph (650 Å×650 Å, illumination from the left) obtained after a dose of 4.1×10^{15} 5 keV Xe^+ ions/m^2 at 300 K. The defect patterns 1 to 5 are discussed in the text. (b) Topograph (1100 Å×1100 Å, grey scale) taken after a dose of 1.9×10^{15} 5 keV Xe^+ ions/m^2 at 300 K and subsequent Pt vapor phase deposition of 0.08 ML at 300 K with a deposition rate of 2.6×10^{-4} ML/s. Inset: scheme of a single dark star.

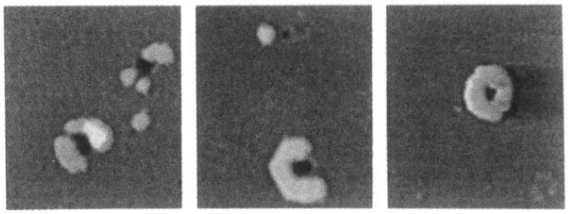

FIG. 3. 5 keV xenon impacts, each causing 400 to 600 atoms to become adatoms (260 Å×220 Å, right topograph: illumination from the left; others: grey scale). Note also a second layer adatom island in left topograph.